https://doi.org/10.5194/egusphere-2024-923
Preprint. Discussion started: 26 April 2024

Coupling the regional climate model ICON-CLM v2.6.6 into the Earth system model GCOAST-AHOI v2.0 using OASIS3-MCT v4.0

Ha Thi Minh Ho-Hagemann[1], Vera Maurer[2], Stefan Poll[3], Irina Fast[4]

[1]Institute of Coastal Research, Helmholtz-Zentrum Hereon, Geesthacht, Germany (Ha.Hagemann@hereon.de)

[2]Deutscher Wetterdienst, Germany

[3] Institute of Bio and Geosciences Agrosphere (IBG-3), Forschungszentrum Jülich, Jülich, Germany; CASA-SDL Terrestrial Systems, Jülich Supercomputing Centre (JSC), Jülich, Germany

[4]German Climate Computing Center (DKRZ), Hamburg, Germany

Correspondence to: Ha Thi Minh Ho-Hagemann, Ha.Hagemann@hereon.de

Abstract

Interactions and feedback between compartments of the Earth system can have a significant impact on local and regional climate and its changes due to global warming. These effects can be better represented by regional Earth system models (RESMs) than by traditional stand-alone atmosphere and ocean models. Here, we present the RESM GCOAST-AHOI version 2.0, which includes a new atmospheric component, the regional climate model ICON-CLM, which is coupled with the ocean model NEMO and the hydrological discharge model HD via the OASIS3-MCT coupler. The GCOAST-AHOI model has been developed and applied for climate simulations over the EURO-CORDEX domain. Two 11-year simulations from 2008-2018 of the uncoupled ICON-CLM and GCOAST-AHOI give similar results for seasonal and annual means of near-surface air temperature, precipitation, mean sea level pressure and wind speed at 10 m height. However, GCOAST-AHOI has a cold SST bias of 1-2 degrees over the Baltic and the North Seas, most pronounced in winter and spring seasons. A possible reason for the cold SST bias could be the underestimation of the downward shortwave radiation at the surface of ICON with the current model settings. Despite of the cold SST bias, GCOAST-AHOI was able to capture other key variables such as those mentioned above well. Therefore, GCOAST-AHOI can be a useful tool to apply for long-term climate simulations over the EURO-CORDEX domain. The new OASIS3-MCT coupling interface OMCI implemented in the ICON-CLM model makes the ICON-CLM model more flexible to couple with an external ocean model and an external hydrological discharge model. Using OMCI, it is also possible to set up a RESM for other regions, such as the Mediterranean Sea.

Keyword: GCOAST, ICON-CLM, OASIS3-MCT coupling interface, climate simulations, EURO-CORDEX, RESM

1 Introduction

GCOAST (Geesthacht Coupled cOAstal model SysTem) is an Earth system framework developed at Helmholtz-Zentrum Hereon, Germany (Staneva et al., 2018). GCOAST is a modular system of different models each developed for a specific component of the Earth system. Based on a specific scientific question, different models from GCOAST can be selected. These models can be plugged together by various couplers, such as OASIS3-MCT (Valcke et al., 2015), ESMF (Earth System

https://doi.org/10.5194/egusphere-2024-923
Preprint. Discussion started: 26 April 2024

Modeling Framework; Hill et al., 2004), or FABM (Framework for Aquatic Biogeochemical Models; https://fabm.net). The coupling can be done at different levels of coupling granularity and the couplers handle the exchange of information between model combinations, individual models, and processes.

GCOAST systems have been applied for several studies covering the Baltic and-North Sea region and part of the North Atlantic. These studies include atmosphere-river-ocean-sea ice coupling (Ho-Hagemann et al., 2020), atmosphere-wave coupling (Wahle et al., 2017; Wiese et al., 2019, 2020), wave-ocean coupling (Staneva et al., 2016; Schloen et al., 2017; Lewis et al., 2019), hydrosphere-biosphere coupling for the Elbe estuary (Pein et al., 2019), the total organic carbon-macrobenthos coupling model (Zhang et al., 2019), and multi-model couplings developed by Lemmen et al. (2018), which have been applied to assess ecosystem impacts of offshore wind farms (Slavik et al., 2019).

So far, the atmospheric model component of GCOAST has been the non-hydrostatic limited area atmospheric model COSMO-CLM v5.0 (Rockel et al., 2008). The COSMO (COnsortium for Small-scale MOdeling) model was initially developed by the Deutscher Wetterdienst (DWD, the German Meteorological Service) in the 2000s as a limited-area weather forecast model. Later, it was further developed in the Climate Limited-area Modeling Community (CLM-Community) as the regional climate model COSMO-CLM (hereafter referred to as CCLM).

In 2001, a cooperation between the DWD and the Max-Planck Institute for Meteorology (MPI-M) was initiated, with the aim of developing a new modelling system for weather prediction and climate simulations. As one result of this initiative, the global numerical weather prediction model ICON (Icosahedral Nonhydrostatic) was developed (Zängl et al., 2015). ICON can also be used in a configuration with regional grid refinement (2-way nesting) or in limited area mode.

In general, two different physics packages are available in ICON: the first one is the Numerical Weather Physics package of DWD (i.e. the ICON-NWP model); and the second one is the ECHAM physics package of MPI-M. In the second package, the global atmospheric model ICON-A (Giorgetta et al., 2018) is coupled with the global ocean model ICON-O (Korn, 2017) and the land and biosphere model JSBACH (Reick et al., 2021) within the ICON Earth System Model (ICON-ESM; Jungclaus et al., 2022). ICON can also be used for large-eddy simulations (Dipankar et al., 2015). ICON-LAM is the Limited-Area Mode of ICON-NWP. Starting in 2017, DWD and the CLM-Community decided to develop the climate limited area mode (ICON-CLM, Pham et al., 2021) based on ICON-LAM.

Nowadays, with contributions from the Karlsruhe Institute of Technology (KIT) and the German Climate Computing Center (DKRZ), the ICON-ESM can include not only the atmospheric, land, river routing, ocean-sea ice and biogeochemical compartments but also the Aerosols and Reactive Trace

https://doi.org/10.5194/egusphere-2024-923
Preprint. Discussion started: 26 April 2024

gases (ART) model. ICON can be set up to operate on several high-performance computing systems such as Bull ATOS at DKRZ (Hamburg, Germany), NEC-Aurora Tsubasa at DWD (Offenbach, Germany) or BullSequana at Forschungszentrum Jülich (FZJ, Jülich, Germany). ICON can be used on a wide range of scales from climate projection, climate prediction and numerical weather prediction down to large-eddy simulations (Heinze et al., 2017). In addition to the main components of the climate system, ICON uses YAC (Yet Another Coupler; Hanke et al., 2016) to couple them.

To couple ICON to an external ocean model such as the NEMO model (Nucleus for European Modelling of the Ocean, Madec et al. 2017), which represents the ocean and sea ice components within GCOAST, there were two feasible options: either to implement YAC interfaces in NEMO, or to implement OASIS interfaces in ICON. Implementing and maintaining YAC interfaces within NEMO is a major challenge. The NEMO model is already linked to the OASIS coupler, which can be used to couple with many other model components. There is no obvious need for YAC interfaces in the NEMO users and developers community. Therefore, it was decided to port the OASIS coupling interfaces from CCLM to ICON-CLM.

For regional ocean-atmosphere coupling over the Baltic Sea, Bauer et al. (2021) have implemented the ESMF interfaces in an earlier version of ICON-NWP as well as into the ocean model GETM. However, they did not consider sea ice in the coupling. ICON-O is the global ocean model of the ICON family and could potentially replace NEMO within GCOAST, but it is not yet available as a regional ocean model for coupling with ICON-CLM.

ICON-NWP/ICON-CLM already includes the land surface schemes TERRA and JSBACH, which are coupled via subroutine to the atmospheric component. However, it might be desirable to couple with other land surface models such as the Community Land Model (CLM), as has been done for the CCLM via the OASIS interface (see Shrestha et al., 2014; Will et al., 2017). There is an ongoing work at FZJ to couple ICON-CLM with the Community Land Model (CLM) via the OASIS3-MCT coupler (in preparation).

The aim of this article is to give a detailed description of the OASIS3-MCT coupling interface (hereafter referred to as OMCI) in ICON (release version 2.6.6), how to implement OMCI with as little modification of the ICON source code as possible, how to compile it on the high-performance computing system Levante at DKRZ, and how to run the coupled system model GCOAST-AHOI with ICON for climate simulations over the EURO-CORDEX domain. This information is useful to other groups planning to couple ICON with NEMO or any other ocean model that already has an available OASIS3-MCT interface. The Earth System Modelling (ESM) Community agrees that ICON and IFS (coupled to FESOM and NEMO) will play a central role within the Helmholtz Association of German

https://doi.org/10.5194/egusphere-2024-923
Preprint. Discussion started: 26 April 2024

Research Centres (HGF). This new OMCI opens more opportunities to use ICON in ESM applications as well as in other modelling communities. The OMCI can also be applied to couple with a land surface model with minor necessary adaptations.

We briefly introduce the coupled system model GCOAST-AHOI in Section 2, and describe the details of OMCI in ICON-CLM in Section 3. Experiment setups are presented in Section 4, followed by an analysis of the model simulations in Section 5. Finally, conclusions and a discussion are given in Section 6.

2 The coupled system model GCOAST-AHOI

GCOAST-AHOI is a subset of GCOAST that includes model components for **A**-Atmosphere and Land, **H**-Hydrological discharge, **O**-Ocean, and **I**-Sea Ice. GCOAST-AHOI version 1.0 (Ho-Hagemann et al., 2020) contains the atmospheric model CCLM v5.0, the ocean model NEMO v3.6 (including the sea ice model LIM3) and the hydrological discharge model HD v4.0 (Hagemann and Dümenil, 1998; Hagemann et al., 2020), coupled via OASIS3-MCT v2.0. A detailed description of CCLM, NEMO and HD as components of GCOAST-AHOI can be found in Ho-Hagemann et al. (2020).

In the GCOAST-AHOI version 2.0, ICON-CLM replaces CCLM as atmospheric model, which is coupled to NEMO v3.6 and HD v5.1 via OASIS3-MCT v4.0. By coupling the atmosphere-ocean-river runoff models in GCOAST-AHOI, we aim to close the water balance in the RESM. Figure 1 illustrates the three models exchanging radiation, wind, pressure, temperature, humidity, water, and sea ice related variables at their interfaces via the OASIS coupler.

https://doi.org/10.5194/egusphere-2024-923
Preprint. Discussion started: 26 April 2024

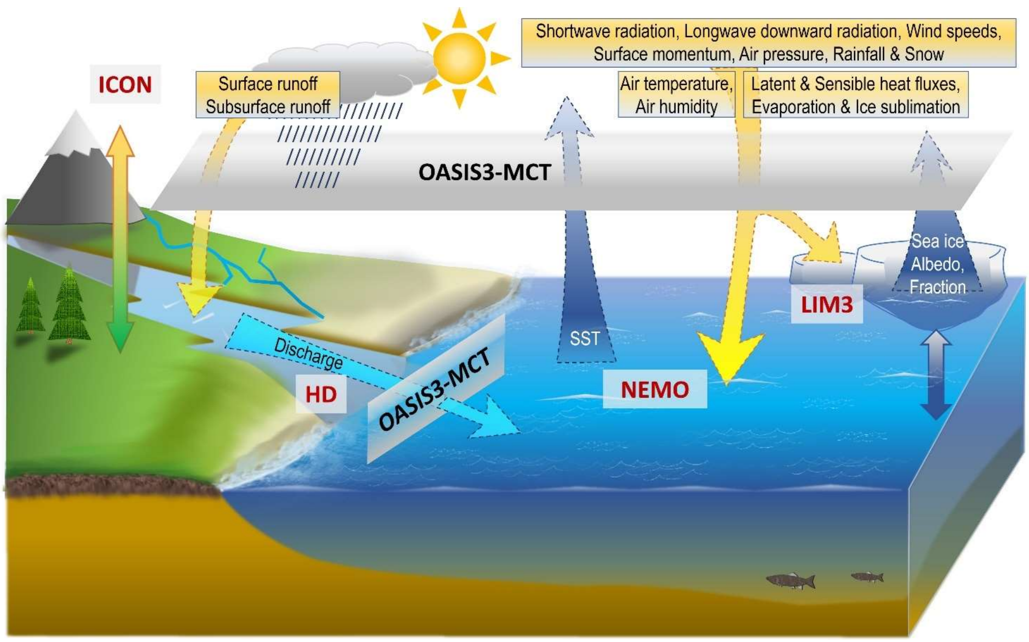

Figure 1: Model components of GCOAST-AHOI and variables exchanged via the OASIS3-MCT coupler. Two solid arrows display the communication between atmosphere-land (yellow-green arrow) and ocean-sea ice (gray-blue arrow), which is done via subroutines inside ICON and NEMO, respectively. Dotted arrows show the transfer between components via the OASIS interface. Yellow arrows present atmospheric transfer to ocean-sea ice and river runoff. The cyan arrow shows the discharge from the river to the ocean. Blue arrows demonstrate the transfer of sea surface temperature (SST) from the ocean as well as the sea ice albedo and sea ice fraction to the atmosphere.

The OMCI in NEMO v3.6 has been modified compared to the original one in the officially released version at http://forge.ipsl.jussieu.fr/nemo/wiki/Users/release-3.6 to be able to receive state variables from the atmospheric model (Ho-Hagemann, 2024). Supplement S1 contains a flowchart of the OMCI for NEMO v3.6. This flowchart differs slightly from Figure 9 in Will et al. (2017), who used the older version NEMO v3.3. The OMCI in HD can be found in the source code publication of Hagemann and Ho-Hagemann (2021). Supplement S2 shows the OMCI of HD. In this article, we describe in detail the OMCI in ICON-CLM, or ICON for short.

In Section 3, we demonstrate the construction of the OMCI in ICON and the optional coupling methods between ICON and NEMO.

3 The coupling OASIS3-MCT interface in ICON

3.1 Interface structure

Figure 2 shows a flowchart of ICON with the OMCI implemented for coupling with NEMO and HD. 10 levels of ICON's source code are described: the first level is the main program ICON, the second

https://doi.org/10.5194/egusphere-2024-923
Preprint. Discussion started: 26 April 2024

level starts with the *start_mpi*, then *atmo_model* and ends with *stop_mpi*, etc.

Levels 2 to 6, 8 and 9 comprise subroutines of ICON (marked in red) that are modified by the coupling. On levels 3 to 7 and 10, new subroutines (orange boxes B1-B7) have been added with the OMCI. They are organized in three modules (cpl_oas_vardef.f90, cpl_oas_mpi.f90 and cpl_oas_interface.f90) containing about 3000 lines of Fortran code (including the current debug lines). The files have been added to the icon/externals/oasis3-mct directory and linked to the src/atm_phy_nwp directory of the ICON source tree.

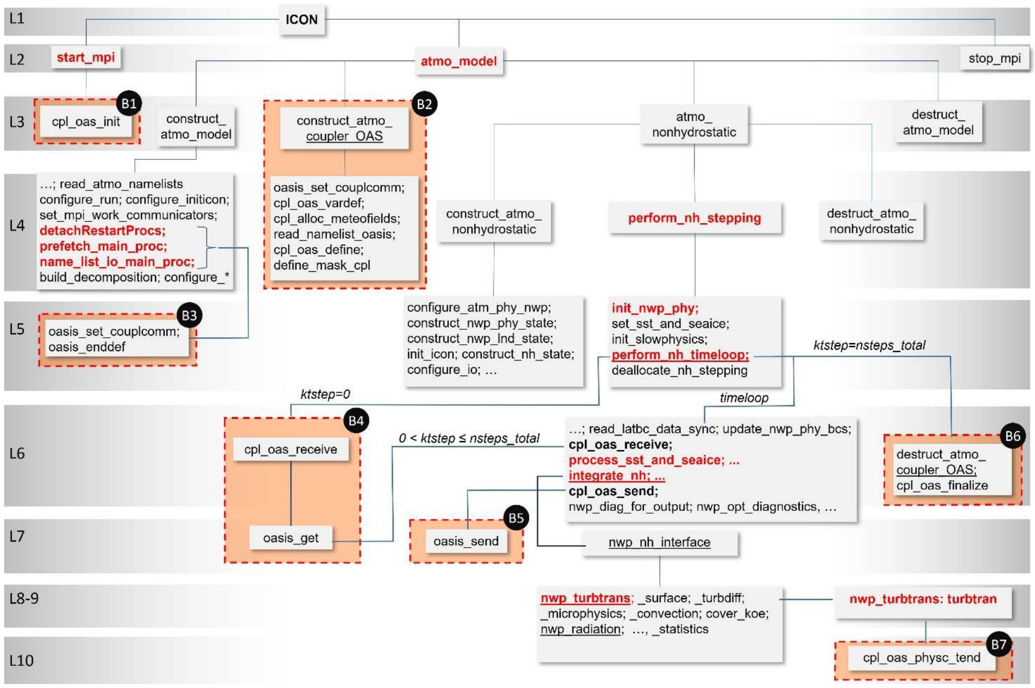

Figure 2: Flowchart of ICON-NWP/ICON-CLM with the OASIS3-MCT coupling interface OMCI. The running sequence is from top to bottom, and from left to right. "L1" indicates the Level 1 – main program ICON, etc. At the levels 2 to 6, 8 and 9, subroutines (in red text) of ICON are modified by the coupling. At the levels 3 to 7 and 10, subroutines added for OMCI are shown in orange boxes (B1-B7).

We can divide the OMCI into four main processes: *Initialization*, *Definition*, *Data exchange*, and *Finalization*. Box B1 (Fig. 2) belongs to the *Initialization* phase of OASIS in ICON. In this phase, the ICON file mo_mpi.f90 is modified, and the file cpl_oas_mpi.f90 of OMCI is newly created (see Supplementary Tables S1 and S2). In mo_mpi.f90, the *start_mpi* subroutine from ICON calls the *cpl_oas_init* subroutine from OMCI, which in turn calls two subroutines from the OASIS library (*oasis_init_comp* and *oasis_get_localcomm)*. The subroutine *cpl_oas_init* (belonging to cpl_oas_mpi.f90) is similar to the subroutine *oas_cos_init* of the unified OASIS interface in CCLM

https://doi.org/10.5194/egusphere-2024-923
Preprint. Discussion started: 26 April 2024

(Will et al., 2017).

Boxes B2 and B3 belong to the *Definition* phase to define and allocate all coupling fields. In this phase, three ICON files are slightly modified by calling *oasis_set_couplcomm* and *oasis_enddef* from the OASIS library (rows 3-5 in Table S2). In addition, some code lines are added to three ICON modules to declare the new sea ice albedo variable “alb_si_ext” to be sent to NEMO (row 6 Table S2).

Two additional files from OMCI (cpl_oas_vardef.f90 and cpl_oas_interface.f90) are added to the ICON source code. Module *cpl_oas_vardef* simply contains a definition of all coupling variables. Part of the *cpl_oas_interface* module is the *construct_atmo_coupler_OAS* subroutine which is called by the ICON *atmo_model* subroutine (src/drivers/mo_atmo_model.f90). The subroutine *construct_atmo_coupler_OAS* also calls *oasis_set_couplcomm* before calling three other subroutines of OMCI (i.e. *read_namelist_oasis*, *oasis_atm_define* and *define_mask_cpl*) to define the decomposition of ICON and to read in the ocean domain masked on the atmospheric domain of ICON (i.e. the coupling mask, variable *mask_cpl*) from a netcdf file named *atmin.nc*.

Calling *oasis_set_couplcomm* in the *Definition* phase is a peculiarity of ICON compared to CCLM, NEMO and HD. The reason for this is that ICON devotes one processor out of the total number of processors to reading the lateral boundary conditions (by setting *num_prefetch_proc=1* in ICON’s parallel_nml namelist). This single processor should be seen by OASIS, but only in the *Initialization* phase. The OASIS subroutine *oasis_set_couplcomm*, called after the *Initialization*, helps to set a coupling communicator in the case that only a subset of the component processes is involved in the coupling. In this case, the “subset” is all the processors allocated for ICON except the one defined by *prefetch_proc*. In the ICON-CLM versions prior to 2.6.4, it is possible to set *num_prefetch_proc=0*, so that the call to *oasis_set_couplcomm* in the *Definition* phase would not be necessary. However, since version 2.6.4, *num_prefetch_proc=1* is mandatory. Therefore, *oasis_set_couplcomm* must be called, otherwise the coupled model will hang after the *Initialization*.

The exchanged variables (see Fig. 1) are listed in the OMCI subroutine *oasis_atm_define* which are read in from a namelist file *namelist_cpl_atm_oce* to define which variables are sent and received. The variable names used in ICON, corresponding to the exchanged variables, are similar to the variables listed in Table 1 of Bauer et al. (2021).

Boxes B4, B5, and B7 belong to the *Data exchange* phase while the coupled system is running. In this phase, subroutines in the OMCI module *cpl_oas_interface* are used, and five ICON modules are modified (rows 7-9 Table S2). The five ICON modules are highlighted in red in Fig. 2 from level 4 to 9, under the subroutine *perform_nh_stepping*. Variables (i.e. sea surface temperature, sea ice

https://doi.org/10.5194/egusphere-2024-923
Preprint. Discussion started: 26 April 2024

fraction and albedo) received from NEMO via OMCI by calling the subroutine *cpl_oas_receive* are updated to the newer values at each ICON time step within the subroutine *perform_nh_timeloop* through several steps. They are first updated in the subroutine *process_sst_and_seaice*, and then used to modify the surface roughness in the turbulent scheme via the subroutine *turbtran* (turb_transfer.f90) of ICON. The subroutine *turbtran* is called by the module *nwp_turbtrans*, which in turn is called by the subroutine *nwp_nh_interface* inside the subroutine *integrate_nh*. After the subroutine *integrate_nh*, the subroutine *cpl_oas_send* is called to pass the defined exchange variables from ICON to NEMO and HD via OMCI.

Box B6 in Fig. 2 indicates the *Finalization* phase for OASIS. Here, two subroutines *destruct_atmo_coupler_OAS* and *cpl_oas_finalize* are called. The subroutine *destruct_atmo_coupler_OAS* simply deallocates all coupling variables. OMCI's subroutine *cpl_oas_finalize* calls two OASIS subroutines *oasis_atm_finalize* and *oasis_terminate*, as in the *Finalization* phase in CCLM, NEMO and HD. Alternatively, the *Finalization* box can be placed at level 3, before *destruct_atmo_model* of ICON. However, leaving the *Finalization* box at level 6 is more flexible, e.g. for testing the behavior of ICON when finalizing OASIS at the *ktstep=nsteps_total* or *ktstep=nsteps_total-1*.

Supplement S4 contains a guide for compiling ICON with this OMCI on Levante at DKRZ. The preparation of OASIS input files for GCOAST-AHOI is described in Supplement S5, which is accompanied by an example of the namcouple file in Supplement S6 and the namelist_cpl_atm_oce in Supplement S7. The command to run GCOAST-AHOI on Levante is provided in Supplement S8. The complete package to conduct experiments for this study is included in the Starter Package for ICON-CLM Experiments (SPICE; Rockel and Geyer, 2022), which is a workflow engine to easily perform long-term simulations. This tool has been further developed from the ICON-CLM_SP starter package (Pham et al. 2021). Some additional parts for coupling with NEMO and HD have been added to the original package.

3.2 Coupling methods

In the officially released version of NEMO v3.6, several fluxes and variables, including shortwave (SW) and longwave (LW) radiation fluxes, latent (LH) and sensible heat (SH) fluxes, rain, snow, evaporation, ice sublimation, mean sea level pressure (MSLP) and surface momentum, can be sent from an atmospheric model to NEMO via the OASIS3-MCT coupler. To be able to receive state variables from the atmospheric model, the OMCI in NEMO v3.6 has been modified to allow air temperature and air specific humidity at 2 m height (T_2M and QV_2M respectively) to be sent from the atmospheric model to NEMO. This allows NEMO to use these variables to calculate the LH and

https://doi.org/10.5194/egusphere-2024-923
Preprint. Discussion started: 26 April 2024

SH, as in the case of the stand-alone NEMO using the "CORE bulk formulae" (Large and Yeager, 2004). Thus, we have three options for the coupling method between ICON and NEMO:

a) CPL_flx: **flux coupling**, which is the default option in the NEMO source code (described above)

b) CPL_var: **state variable coupling**, the new method, where SW and LW, T_2M, QV_2M, wind speed at 10 m height (UV_10M), rain, snow, MSLP, surface momentum are sent from ICON to NEMO. NEMO calculates LH and SH using the "CORE bulk formulae" which is based on the Monin Obukhov similarity theory.

c) CPL_mix: **mixture coupling**, the new method, like CPL_var, but ICON also sends LH and SH to NEMO. NEMO then averages them with the LH and SH calculated using the "CORE bulk formulae".

With the modification of OMCI in NEMO v3.6, it is now easy to select the coupling method via the namelist settings. Section 5 considers the simulations using the coupling method 3 (CPL_mix), which was also used in Ho-Hagemann et al. (2020).

In turn, NEMO sends the sea surface temperature, sea ice fraction and sea ice albedo to ICON. Fig. 3 illustrates how the surface temperature is updated in ICON over the ocean (left side) and over land (right side) in the presence of sea ice and snow. ICON utilizes a tile approach to compute surface fluxes of momentum and scalars. For the "sea-water type" grid boxes, the grid box mean fluxes are computed as a weighted average of the fluxes over ice and over open water, using the fractional ice cover *fice* and the fractional open water cover (*1 – fice*) as the respective weights. Sea ice in each ICON grid box is considered only if *fice* exceeds its minimum value of 0.015. Otherwise, the grid box is treated as ice-free. In ICON, two types of surface temperature are considered: the ground temperature t_g and the surface temperature t_s. If a grid box is covered by sea ice or snow, t_g is the mixed temperature of the free sea ice/free snow surface temperature and the temperature on top of the sea ice/snow. Under the sea ice, t_s is calculated as a mixture of the free sea ice temperature and the salt water freezing temperature of 271.45 K. If there is no sea ice or snow in the grid box, t_g is equal to t_s. In principle, NEMO can send the mixed sea ice and water temperature to ICON to update t_g over the ocean points, as in CCLM in Ho-Hagemann et al. (2020). Or it can send the open water temperature, the sea ice surface temperature and the sea ice fraction so that ICON can calculate t_g as the mixture. However, in the uncoupled mode of the current ICON-CLM version, the sea surface temperature (SST) forcing is read in as the variable t_seasfc (or t_s_w in Fig. 3) and passes through the subroutines *nwp_surface_init* and *process_sst_and_seaice* to calculate t_g. To be consistent with the ICON-CLM updates, we pass the SST (to update the t_seasfc), the sea ice fraction (to update fr_seaice), and the sea ice albedo (alb_si_ext) from NEMO to ICON.

https://doi.org/10.5194/egusphere-2024-923
Preprint. Discussion started: 26 April 2024

ICON will then calculate t_g, t_s, alb_si, etc. using its sea ice scheme. In the future, we may modify this coupling method by using the sea ice temperature from NEMO.

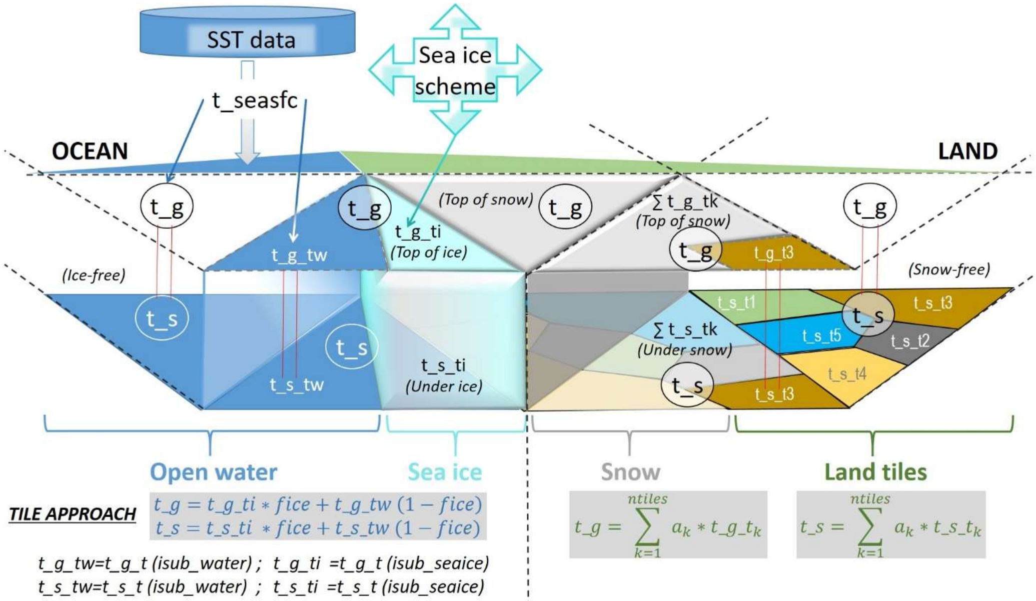

Figure 3: Surface temperature exchange between atmosphere and ocean/land in ICON and GCOAST-AHOI.

4 Experimental design

In this study, two experiments are conducted with the uncoupled ICON (ICON266) and GCOAST-AHOI (ICPL266) for the period of 2008-2018. An experiment starts on 01 January 2008 and ends on 01 January 2019, restarting each month. The integration domains of ICON, NEMO and HD are displayed in Fig. 4. The namelist setup of physical parametrization for ICON-CLM is similar to that of the NUKLEUS project (B. Geyer, personal communication). The resolution of ICON is R13B5, with an approximate mesh size of 12 km, using 60 vertical levels. The model top height is at 23.5 km. The following physical schemes are used in the current namelist setting of ICON: Radiation scheme ecRad (Hogan and Bozzo, 2018; Rieger et al., 2019); Mass-flux shallow and deep convection scheme (Tiedtke, 1989; Bechtold et al., 2008); Microphysics single-moment scheme (Doms et al., 2004); Planetary boundary layer scheme prognostic TKE (Raschendorfer, 2001; Raupach and Shaw, 1982); Land-surface scheme tiled TERRA (Schrodin and Heise, 2001; Schulz et al., 2016; Schulz and Vogel, 2020). The initial and lateral boundary forcing of ICON is obtained from the ERA5 reanalysis data (Hersbach et al., 2020). The Tegen aerosol climatology (Tegen, 1997), i.e. a monthly aerosol optical depth of sulphate droplets, total dust, organic carbon, black carbon, and sea salt, is used in this study. The initial and daily lateral boundary forcing of NEMO is taken from the ORAS5 reanalysis

https://doi.org/10.5194/egusphere-2024-923
Preprint. Discussion started: 26 April 2024

data (Copernicus Climate Change Service, 2021). The spatial resolution of NEMO is ~3.7 km with 50 vertical levels. HD has the resolution of 1/12 degrees, ca. 8 km. More information on the model configuration can be found in Table 1 and in Ho-Hagemann et al. (2020).

Table 1: Model configuration

Configuration	ICON	NEMO	HD	Coupler OASIS3-MCT
Version	v2.6.6	v3.6	v5.1	V4.0
Domain	EURO-CORDEX	North Sea, Baltic Sea, North Atlantic	Europe	-
Resolution	~ 12 km	~ 3.7 km	~ 8 km	-
Grid points	231660	902 x 777	960 x 540	
Time step	100 s	90 s	3600 s	3600 s
Forcing	ERA5	ORAS5, OTIS	-	-

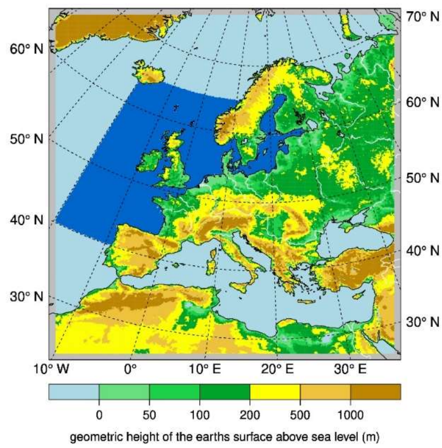

Figure 4: Integration domains of ICON and HD (EURO-CORDEX) and of NEMO-LIM3 (dark blue).

To estimate the computational performance of the coupled model, we used LUCIA (Maisonnave and Caubel, 2014), which is part of OASIS3-MCT. In Supplement S9, we describe how to use LUCIA for GCOAST-AHOI. In this study, we conduct five one-month experiments using ICPL266 to find out the most suitable number of nodes used for each model component. The five experiments are carried out with different numbers of nodes (i.e. 25 nodes, 30 nodes and 40 nodes). The number of processors assigned to each model component is listed in Table 2.

Table 2: Number of requested nodes/processors for performance tests of GCOAST-AHOI on Levante. NPX and NPY are the processors for NEMO corresponding to x and y dimensions, respectively.

Case	Nodes	Total processors	Processors for ICON	Processors for NEMO	Processors for HD
A	25	3200	1599	NPX x NPY = 40 x 40 = 1600	1
B	30	3840	2239	NPX x NPY = 40 x 40 = 1600	1
C	30	3840	1839	NPX x NPY = 50 x 40 = 2000	1
D	40	5120	3519	NPX x NPY = 40 x 40 = 1600	1
E	40	5120	2719	NPX x NPY = 60 x 40 = 2400	1

https://doi.org/10.5194/egusphere-2024-923
Preprint. Discussion started: 26 April 2024

Figure 5 shows computation time (green bars) and coupling exchange time, including the time spent while waiting for slower models (red bars) of the model components. In principle, the smaller the red bars, the better the computational performance. Also, the red bars of ICON and NEMO should not be too different. As a simpler model, HD runs on a single processor, so its running time (green bar) is the shortest and the waiting time (red bar) the longest of the three models.

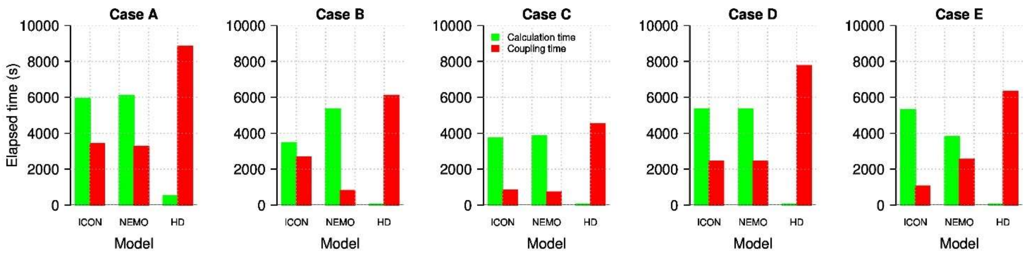

Figure 5: Calculation time (green) versus coupling exchange duration including time spent to wait for other model components (red). See table 2 for a detailed view of the node balance of the displayed cases.

Figure 5 shows that **Case C** is the most balanced of the five experiments. In this case, 30 nodes were used, the number of processors (in short procs) given to NEMO (2000 procs) and ICON (1839 procs) are similar. The green and red bars of ICON and NEMO are similar. In **Case A**, 25 nodes were used, the number of processors given to NEMO (1600 procs) is also very similar to that given to ICON (1599 procs), but the green bars of this case are the highest of the five cases. These two cases have a different ratio of processors used for NEMO. The best one (**Case C**) has NPX x NPY = 50 x 40 while the worst one (**Case A**) has NPX x NPY = 40 x 40. **Case B** also uses 30 nodes like **Case C**, but with NPX x NPY = 40 x 40 = 1600 and ICON uses 2239 processors. With more processors, ICON runs faster than NEMO in this case, so there is no balance. In **Case D** uses 40 nodes, again 1600 processors for NEMO and an increased number of processors (3519 procs) for ICON. Here, ICON runs as slow as NEMO, even though it uses more than twice as many processors as NEMO. **Case E** also uses 40 nodes, but the number of processors for ICON and NEMO are not much different (i.e. 2719 and 2400 procs). However, NEMO runs faster than ICON and the system takes a longer time to run than in **Case C**. ICON with more processors in **Case D** and **Case E** is slower than on **Case B** and **Case C** with less processors, which indicates that too many processors were used. The common recommendation for ICON is to have at least 100 grid cells per processor, which would be about 2000 processors at maximum for the EURO-CORDEX domain. These results indicate that not only the number of the nodes used, but also the ratio of processors between ICON and NEMO, and the ratios of NPX and NPY for NEMO should be chosen carefully. The optimal setup may be different on other computer

https://doi.org/10.5194/egusphere-2024-923
Preprint. Discussion started: 26 April 2024

systems. A more thorough analysis is planned to be done with the new OASIS-MCT_5.0 version of LUCIA.

5 Model simulations

The first two years 2008-2009 are excluded as spin-up time, and the output data of the two simulations ICON266 and ICPL266 for nine years (2010-2018) are compared with the observational and ERA5 data to assess the model performance. For sea surface temperature (SST), we use the Operational Sea Surface Temperature and Ice Analysis (OSTIA) data (Good et al. 2020) to evaluate the simulated SST of ICPL266. For air temperature at 2 m height (T_2M) and precipitation (TOT_PREC), the daily E-OBS data (Haylock et al. 2008; Van den Besselaar et al. 2011) version 27.0 on the grid of 0.11 degree are used. The ERA5 reanalysis data are interpolated onto the E-OBS grid and used as a reference for comparison with the simulated shortwave and longwave surface radiation, mean sea level pressure (PMSL), wind speed at 10 m height (SP_10M), and T_2M. The Surface Radiation Data Set - Heliosat (SARAH) - Edition 2 (Pfeifroth et al. 2017) is used to evaluate the shortwave downward radiation of the simulations.

Seasonal means of winter (DJF), spring (MAM), summer (JJA), autumn (SON) and annual means (ANN) of several variables are analysed. Over the ocean, the sea surface temperature (SST) of ICON266 is the ERA5 forcing data, which is based on observations, so it's very close to the OSTIA data (not shown). Thus, the SST difference between the coupled and the stand-alone run (Fig. 6) can be interpreted as a bias towards a measurement-based product. In the coupled model, the SST is provided by NEMO over the GCOAST domain. In general, ICPL266 has a cold SST bias of about 1-3 degrees over the GCOAST domain, except around the British coast in summer (JJA, Fig. 6).

The cold SST bias of ICPL266 over the GCOAST domain may intensify the cold T_2M bias (Fig. 7b, Fig. S1), especially in winter (DJF) and spring (MAM). In summer, ICPL266 reduces the warm T_2M bias of ICON266 (Fig. 7a). In general, the annual (ANN) T_2M bias of ICPL266 is slightly colder (e.g. 0.5°C) than that of ICON266. Comparison with the E-OBS data (Fig. S2) shows similar results to Fig. 7, except over Nothern Africa and Turkey, where the quality of the E-OBS data is affected by the lack of observations in that region (cf. Fig. 1 in Hagemann and Stacke, 2022).

A possible reason for the SST cold bias of ICPL266 may be that the shortwave and longwave radiation from ICON sent to NEMO is too low. Figure S3 shows the relative bias (%) of the shortwave downward radiation (SWDN) of ICON266 and ICPL266 compared to the ERA5 data, as well as the relative difference (%) between SARAH2 and ERA5. Figure 8 shows a zoomed section of Fig. S3 over the GCOAST ocean domain. In general, both ICON266 and ICPL266 have a positive SWDN bias of less

https://doi.org/10.5194/egusphere-2024-923
Preprint. Discussion started: 26 April 2024

than 10 % over land compared to ERA5, except 15-20 % over northern Europe in winter and eastern Europe in autumn (Fig. S3). Over the North Sea, ICON266 and ICPL266 have a small negative bias of about 5-10 % compared to ERA5 (Fig. 8). The area of negative SWDN bias in the North Sea is slightly larger in ICPL266 than in ICON266. Comparing the ERA5 data and the SARAH2 data, SWDN over southern Europe is similar between the two datasets, with SARAH2 being slightly larger over land (Fig. S3). In general, the SWDN of ICON266 and ICP266 over the North Sea is rather close to the SARAH2 data, but slightly overestimated over the Baltic Sea.

Figure S4 in the Supplementary Appendix shows a similar plot to Fig. S3, but for the longwave downward radiation (LWDN) and without the SARAH2 data, as it is not available. The modeled LWDN has a negative bias of about 2-4 % annually and a larger bias in winter of about 6-8 %, most pronounced over land. Over the ocean, ICON266 reproduces well the LWDN of the ERA5 data, and ICPL266 has a small negative bias of 2-4 %.

The namelist settings of the NEMO model used in this study were tuned to the ERA5 forcing data in the uncoupled mode. The annual mean SST bias of the stand-alone NEMO is less than 0.5 degrees over the Baltic and North Seas, and of about -1 to -2 degrees over the North Atlantic compared to the OSTIA data (not shown). In summer, the positive SST bias of about 1-2 degrees is found over the Baltic and North Seas (not shown). In the future, to reduce the cold SST bias over the North Sea in the coupled simulations, we plan to increase the SWDN of ICON by about 10 % before sending it to NEMO. However, the cold SST bias over the Baltic Sea does not seem to be directly related to the SWDN and LWDN. The negative wind speed bias in ICPL266 (Fig. 9) could be another element contributing to the SST bias, which needs to be analyzed in more detail in the future. Otherwise, a short spin-up time of 2 years may be too short for NEMO to reach the stable state, leading to the cold SST bias. In addition, NEMO‘s namelist settings should also be optimized for the coupled simulations.

In the COPAT2 (Coordinated Parameter Testing, phase 2) initiative of the CLM-Community, several parameters of ICON-CLM are being tested in a similar way as done for the COSMO-CLM model (Russo et al., 2024) to find out the recommended settings. For example, the use of the transient aerosol MAC2-SP (Kinne, 2019) and a careful adjustment of various namelist settings related to cloud cover, the soil and vegetation scheme and the turbulent transfer will further reduce the T_2M cold bias and improve the shortwave downward radiation.

https://doi.org/10.5194/egusphere-2024-923
Preprint. Discussion started: 26 April 2024

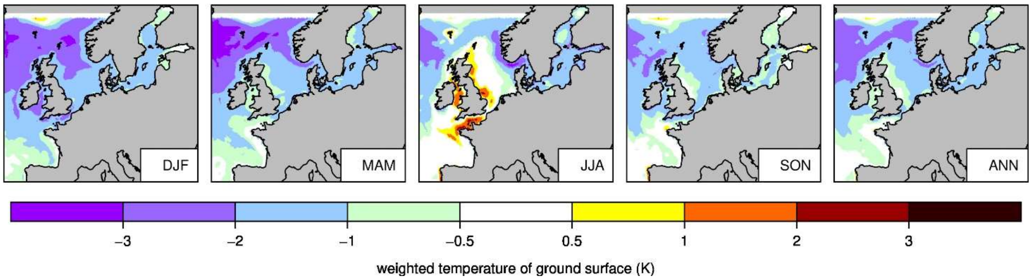

Figure 6: Seasonal (DJF, MAM, JJA, SON) and annual (ANN) mean of sea surface temperature (K) difference between ICPL266 and the OSTIA data for the period of 2010-2018 over the GCOAST domain.

a) ICON266

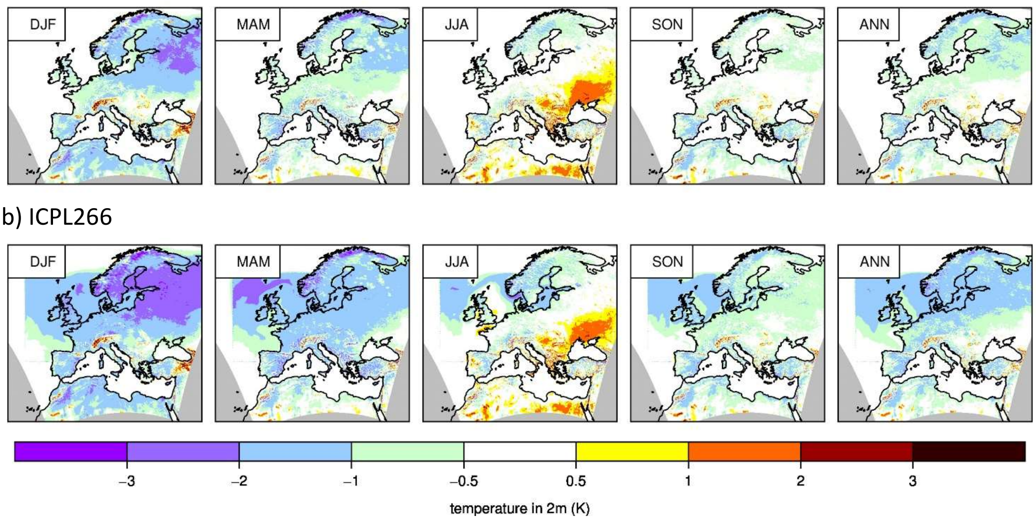

Figure 7: Seasonal (DJF, MAM, JJA, SON) and annual (ANN) of 2m air temperature (K) difference between a) ICON266 and b) ICPL266 compared to the ERA5 reanalysis data for the period of 2010-2018.

https://doi.org/10.5194/egusphere-2024-923
Preprint. Discussion started: 26 April 2024

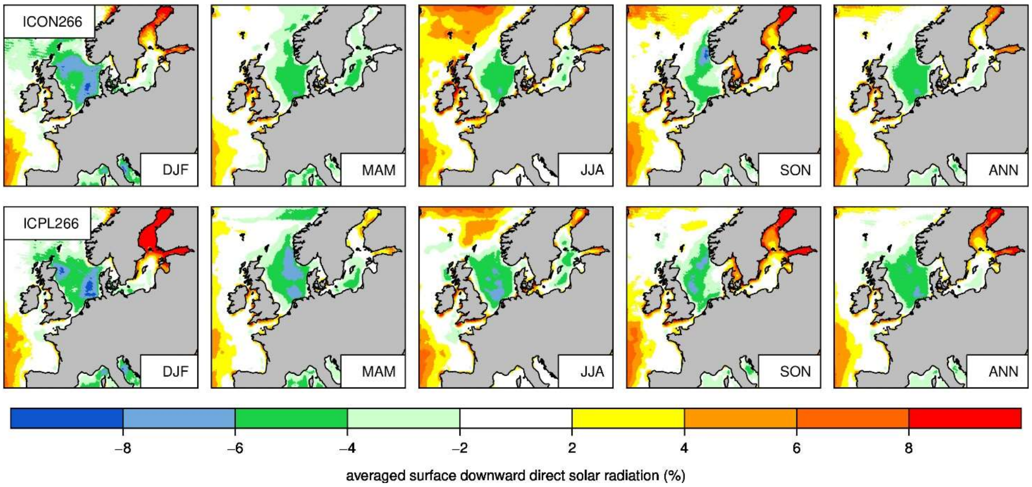

Figure 8: Seasonal (DJF, MAM, JJA, SON) and annual (ANN) of shortwave downward radiation bias (%) of ICON266 (top) and ICPL266 (bottom) compared to the ERA5 data for the period of 2010-2018 over the GCOAST domain.

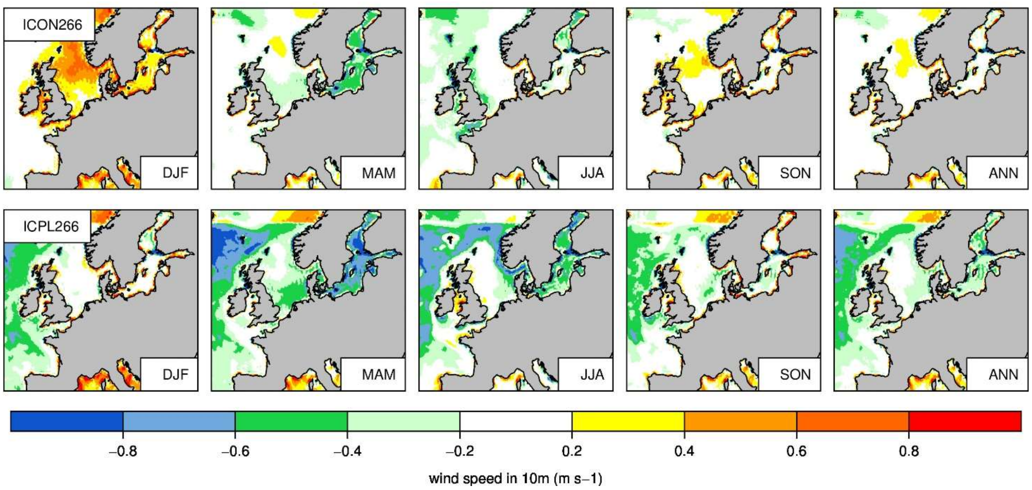

Figure 9: Seasonal (DJF, MAM, JJA, SON) and annual (ANN) 10-M wind speed bias (m s^{-1}) of ICON266 (top) and ICPL266 (bottom) compared to the ERA5 data for the period of 2010-2018 over the GCOAST domain.

The precipitation biases of the two simulations ICON266 and ICPL266 compared to the E-OBS data are very similar with a wet bias in winter and spring and a dry bias in summer (JJA) and autumn (SON, Fig. 10). Fig. S5 and Fig. S6 in the Supplement show the biases of PMSL and SP_10M compared to ERA5. ICPL266 tends to overestimate the PMSL throughout the year except in the summer, while ICON266 has only a pronounced positive bias in winter (DJF) and negative bias in summer (JJA). The wind speed of the two simulations is very similar over land. ICPL266 tends to reduce the wind speed

https://doi.org/10.5194/egusphere-2024-923
Preprint. Discussion started: 26 April 2024

over the GCOAST ocean domain by up to 1.5 m s^{-1} compared to ICON266. This reduction leads to a notable deviation of wind speed from ERA5 over the ocean, except in winter (DJF). Here, ICON266 has a positive bias of about 0.5 m s^{-1} over the North Sea (Fig. S5a), but ICPL266 is very close to ERA5.

a) ICON266

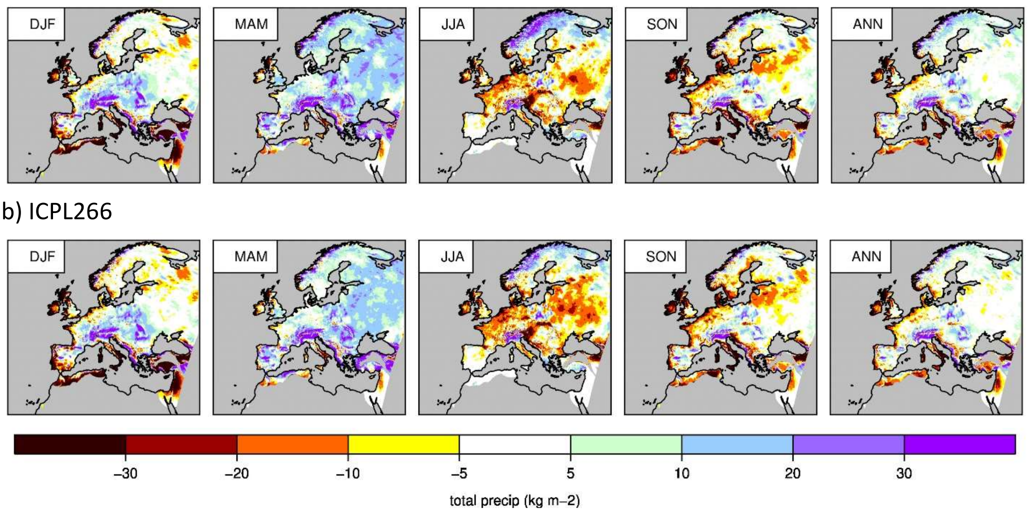

Figure 10: Seasonal (DJF, MAM, JJA, SON) and annual (ANN) difference of precipitation (mm month $^{-1}$) between a) ICON266 and b) ICPL266 compared to the E-OBS data for the period of 2010-2018.

Figure 11 shows monthly climatologies of different variables (T_S, T_2M, TOT_PREC, PMSL) over the GCOAST domain or the whole EURO-CORDEX domain, considering only ocean or land points. ICPL266 has a cold T_S bias of about 1-2 degrees over the ocean (Fig. 11a), which also causes the T_2M bias of 0.5-1 degrees over the ocean (Fig. 11c). In winter, ICPL266 is slightly colder over land than ICON266 and E-OBS (Fig. 11d). In summer, both simulations are very close to E-OBS. The simulated precipitation of ICON266 tends to be overestimated compared to E-OBS with a maximum in May and June, and slightly underestimated in August and September (Fig. 11b). The coupled run shows 1-3 mm/month less precipitation than the atmosphere-only experiment. In previous studies by Ho-Hagemann et al. (2015, 2017), the stand-alone atmospheric model COSMO-CLM has a dry bias in summer and the coupled run reduces the dry bias due to the improvement of the moisture convergence and transport from ocean to land. This situation is not found in the current study, which needs to be thoroughly analyzed in the future.

For the PMSL, the whole EURO-CORDEX domain is considered, but separately for ocean points (Fig. 11e) and land points (Fig. 11f). In both cases, ICPL266 has a larger PMSL than ICON266. The higher surface pressure in ICPL266 may be caused by the cooler air near the surface (due to the negative T_2M bias) which leads to a higher density of the air mass and therefore a higher pressure.

https://doi.org/10.5194/egusphere-2024-923
Preprint. Discussion started: 26 April 2024

Over the ocean, the PMSL of ERA5 is better reproduced by ICPL266 than by ICON266. Over land, ICPL266 increases the PMSL positive bias in winter compared to ICON266.

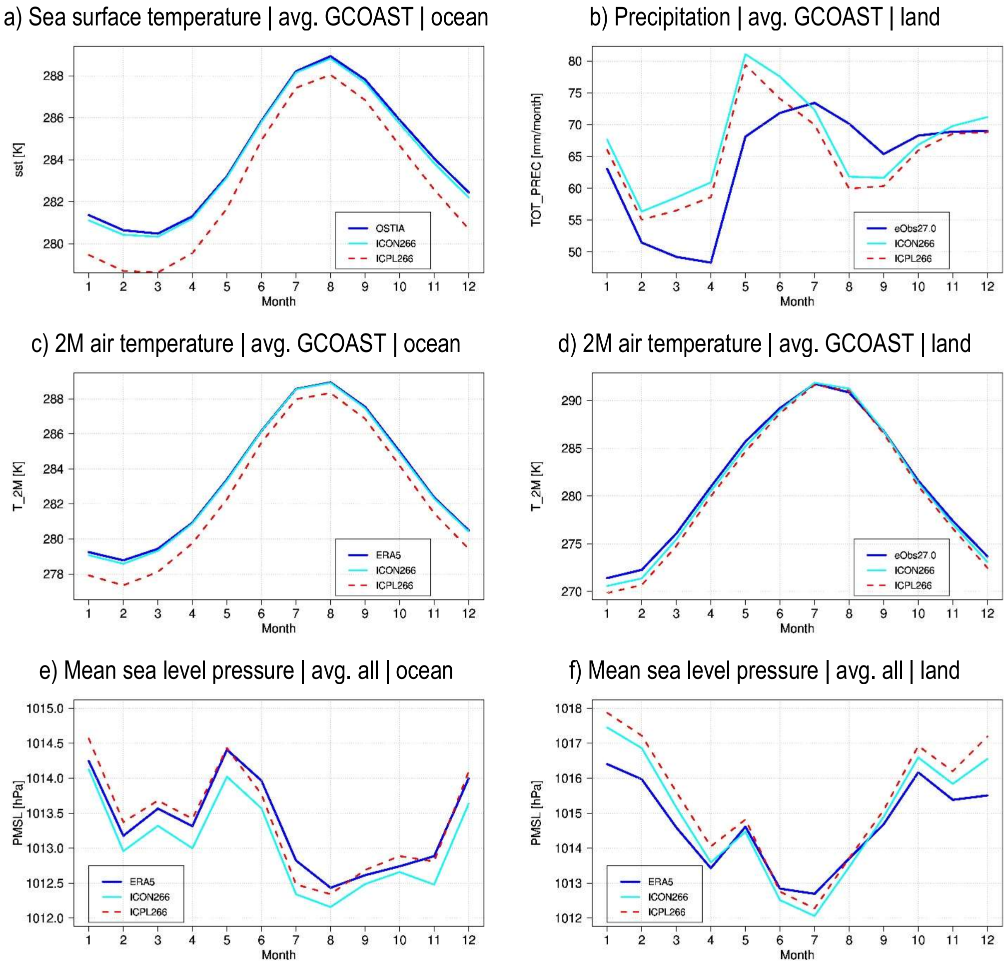

Figure 11: Annual variability of T_S (K), T_2M (K), PMSL (hPa) and precipitation (mm/month) of ICON266 (cyan solid line) and ICPL266 (red dashed line) compared to the OSTIA, ERA5 and E-OBS data (blue solid line) for the period of 2010-2018. Values are averaged over the GCOAST domain (avg. GCOAST) or the whole EURO-CORDEX domain (avg. all), over the ocean or land points only.

Conclusion and Outlook

In the present study, we introduce the regional Earth system model (RESM) GCOAST-AHOI version 2.0, in which a new atmospheric component - the regional climate model ICON-CLM version 2.6.6 - is coupled with the ocean model NEMO version 3.6 and the hydrological discharge model HD version 5.1 via the OASIS3-MCT coupler version 4.0.

https://doi.org/10.5194/egusphere-2024-923
Preprint. Discussion started: 26 April 2024

GCOAST-AHOI v2.0 is developed and applied for climate simulations over the EURO-CORDEX domain. Two 11-year simulations from 2008-2018 of the uncoupled ICON-CLM (ICON266) and GCOAST-AHOI (ICPL266) yield similar results for seasonal and annual means of near-surface air temperature and precipitation, as well as mean sea level pressure and wind speed at 10 m height. However, ICPL266 has a cold SST bias of 1-2 degrees over the Baltic and the North Seas, most pronounced in winter and spring seasons. A possible reason for the cold SST bias could be the underestimation of the downward shortwave radiation at the surface of ICON-CLM with the current model settings. A deeper analysis of the bias will be done in the next study, especially after re-running the simulations with the optimal settings of ICON-CLM, which will be found within the COPAT2 initiative of the CLM-Community. For example, the performance of ICON-CLM will be tuned by using the transient MAC2-SP aerosol data (Kinne, 2019) and modified namelist parameters related to cloud cover to improve the shortwave downward radiation and reduce the cold bias.

Despite the cold SST bias, ICPL266 was able to capture the distribution of temperature, precipitation, mean sea level pressure and wind speed well, similar to the uncoupled ICON-CLM model. The added value of the coupled model compared to the stand-alone model is usually found in the case of extreme events (Ho-Hagemann et al., 2015, 2017, 2020; Wiese et al., 2019, 2020). Therefore, we will analyze the model simulations with a focus on extreme events in the next study.

Our present study shows that the RESM GCOAST-AHOI can be a useful tool for conducting long-term regional climate simulations. The new OASIS3-MCT coupling interface OMCI implemented in the ICON-CLM model makes the ICON-CLM model more flexible to couple with an external ocean model and an external hydrological discharge model, not only with NEMO and HD. Given that the standalone model components for each the atmosphere and the ocean are available for a specific geographical domain, it is also quite easy to apply GCOAST-AHOI to other regions. Besides preparing the lateral boundary conditions for NEMO over the new domain, and the OASIS input files (as described in Supplementary S5 and S6), it is necessary to prepare several new parameter files so that OASIS3-MCT can exchange the discharge from HD to NEMO without interpolation. On the one hand, these are files for the general setup of the HD model. The creation of these files is described in Sect. 3 of the HD model readme mark down file included in the HD model package (Hagemann et al. 2023). On the other hand, this includes the HD model coupling file, which is used for coupling via OASIS. Instructions for its generation are provided in Section 2.1 of a markdown file dedicated to the HD model coupling exercises (Hagemann et al. 2023).

ICON-CLM with OMCI is also used to couple ICON-CLM with NEMO v4.2 over the GCOAST domain (in preparation) and with NEMO-MED v3.6 over the Mediterranean Sea region in the CLM-

https://doi.org/10.5194/egusphere-2024-923
Preprint. Discussion started: 26 April 2024

Community. OMCI for the older ICON version 2.6.4 can be found in Ho-Hagemann (2022).

Recently, the ICON Consortium has developed and released the Community interface (Comin) for the ICON model to allow ICON to be coupled with external model components. In the future, OMCI will be integrated into tComin via a plugin. For example, instead of calling cpl_oas_init in the ICON source code, the start_mpi subroutine of ICON will call e.g. Comin_Init and within the Comin_Init subroutine, the cpl_oas_init will be called. It is similar for other subroutines of OMCI, i.e. they can be called in the Comin interface instead of directly in the main subroutines of ICON as it is currently done. In combination with the external coupler YAC, there will be an easier maintainable code for the coupling interface. Using the ComIn entry points will not require any additional patching of the ICON source code.

Currently, also a limited area mode of the ocean model (ICON-O-LAM) is being developed within the ICON consortium. This can be coupled with ICON-CLM via the YAC coupler in the ICON-Seamless framework. When that RESM will be available in the future and will be applied for the EURO-CORDEX domain, its simulation can be compared with the simulations of GCOAST-AHOI as a good reference. Investigating difference in simulations of the two RESMs could be helpful to understand better the coupling interactions and feedback between model components of the climate system.

Supplementary Materials: Supplementary material is available online together with the submitted manuscript.

Author Contributions: H.T.M. H.-H. developed the OMCI in ICON-CLM and HD, modified the OMCI in NEMO, designed the experiments and carried them out, analyzed the results; H.T.M. H.-H. prepared the manuscript with contributions from all co-authors; V.M. contributed to analyze the simulations; S.P contributed to develop the OMCI in ICON-CLM; I.F. supported debugging the GCOAST-AHOI on the DKRZ HPC system. All authors have read and agreed to the published version of the manuscript.

Funding: This study was conducted within the CoastalFutures project that was funded by the German Federal Ministry of Education and Research under grant number 03F0911E. Moreover, it has been supported by funding from the German project REKLIM. The work described in this article has received funding from the Initiative and Networking Fund of the Helmholtz Association through the project “Advanced Earth System Modelling Capacity (ESM)”. The content of the article is the sole responsibility of the author(s) and it does not represent the opinion of the Helmholtz Association, and the Helmholtz Association is not responsible for any use that might be made of the information contained. The study also contributes to the fourth programm-oriented funding phase (PoF IV) of the Helmholtz Association of German Research Centers.

Acknowledgements: The authors are grateful to the following entities: The German Climate Computing Center (DKRZ) provided the computer hardware for the Limited Area Modelling simulations in the project “Regional Atmospheric Modelling”; We acknowledge the E-OBS dataset from the EU-FP6 project UERRA (http://www.uerra.eu) and the Copernicus Climate Change Service, and the data providers in the ECA20ndD project (https://www.ecad.eu). We

https://doi.org/10.5194/egusphere-2024-923
Preprint. Discussion started: 26 April 2024

appreciate the use of the ERA5 reanalysis product that was provided by the European Centre for Medium-Range Weather Forecasts (ECMWF). ERA5 data reformatted by the CLM community provided via the DKRZ data pool were used. This study has been conducted using E.U. Copernicus Marine Service Information (https://doi.org/10.48670/moi-00165). We express our thanks to CERFACS (France) for the availability of the OASIS3-MCT coupler, especially to Eric Maisonnave for a support with the LUCIA tool in OASIS3-MCT. We thank Sebastian Grayek (formerly at Helmholtz-Zentrum Hereon) for preparing the NEMO lateral boundary conditions. We are also grateful Daniel Rieger and Daniel Reinert (DWD) for their advice on ICON source code. We thank Stefan Hagemann (Hereon) for proving information on setting the HD model. We express our thank to Panagiotis Adamidis (DKRZ) for the great technical support.

Code and data availability: ICON is available to the community under a permissive open source licence (BSD-3C). One can download the newest released version at https://gitlab.dkrz.de/icon/icon-model. The source code of ICON v2.6.6 including the OMCI is published on Zenodo (https://doi.org/10.5281/zenodo.11057794).

The NEMO source code is freely available and distributed under CeCILL license (GNU GPL compatible). To download the NEMO reference version (for now revision 3.6):

svn co http://forge.ipsl.jussieu.fr/nemo/svn/NEMO/releases/release-3.6/NEMOGCM

The modified NEMO v3.6 source code for different coupling methods are published on Zenodo (https://doi.org/10.5281/zenodo.11057794).

The HD source code is available at https://doi.org/10.5281/zenodo.4893099.

Source code of OASIS3-MCT v4.0 with small modifications in lib/psmile/src/GPTLget_memusage.c and lib/mct/mct/m_AttrVectComms.F90 is published on Zenodo (https://doi.org/10.5281/zenodo.11057794).

Input data, run-scripts, evaluation scripts are published on Zenodo (https://doi.org/10.5281/zenodo.11057794). Because of its huge volume, forcing data used for this study is available from the authors upon request.

Conflicts of Interest: The authors declare no conflict of interest. The funders had no role in the design of the study; in the collection, analyses, or interpretation of data; in the writing of the manuscript, or in the decision to publish the results.

References

Bauer, T. P., Holtermann, P., Heinold, B., Radtke, H., Knoth, O., and Klingbeil, K.: ICONGETM v1.0 – flexible NUOPC driven two-way coupling via ESMF exchange grids between the unstructured-grid atmosphere model ICON and the structured grid coastal ocean model GETM, Geosci. Model Dev., 14, 4843–4863, https://doi.org/10.5194/gmd-14-4843-2021, 2021.

Bechtold, P., Kohler, M., Jung, T., Leutbecher, M., Rodwell, M., Vitart, F., and Balsamo, G.: Advances in predicting atmospheric variability with the ECMWF model, 2008: From synoptic to decadal time-scales. Quart. J. Roy. Meteor. Soc., 134, 1337–1351, https://doi.org/10.1002/qj.289, 2008.

Copernicus Climate Change Service, Climate Data Store: ORAS5 global ocean reanalysis monthly data from 1958 to present, Copernicus Climate Change Service (C3S) Climate Data Store (CDS), https://doi.org/10.24381/cds.67e8eeb7, 2021.

Dipankar, A., Stevens, B., Heinze, R., Moseley, C., Zängl, G., Giorgetta, M., and Brdar, S.: Large eddy simulation using the general circulation model ICON, J. Adv. Model. Earth Syst., 7, 963–986, doi:10.1002/2015MS000431, 2015.

Doms, G., and Coauthors: A description of the nonhydrostatic regional model LM. Part II: Physical parameterization. Tech. Rep., Deutscher Wetterdienst, Offenbach, Germany, 146 pp., http://www.cosmo-model.org/content/model/documentation/core/cosmoPhysParamtr.pdf, 2004.

https://doi.org/10.5194/egusphere-2024-923
Preprint. Discussion started: 26 April 2024

Giorgetta, M. A., Brokopf, R., Crueger, T., Esch, M., Fiedler, S., Helmert, J., et al.: ICON-A, the atmosphere component of the ICON EarthSystem Model: I. Model description. Journal of Advances in Modeling Earth Systems. https://doi.org/10.1002/2017MS001242, 2018.

Good, S., Fiedler, E., Mao, C., Martin, M.J., Maycock, A., Reid, R., Roberts-Jones, J., Searle, T., Waters, J., While, J., and Worsfold, M.: The Current Configuration of the OSTIA System for Operational Production of Foundation Sea Surface Temperature and Ice Concentration Analyses. Remote Sens., 12, 720, https://doi.org/10.3390/rs12040720, 2020.

Hagemann, S., and Dümenil, L.: A parametrization of the lateral waterflow for the global scale, Climate Dyn., 14, 17–31, https://doi.org/10.1007/s003820050205, 1998.

Hagemann, S., and Ho-Hagemann, H.T.M.: The Hydrological Discharge Model - a river runoff component for offline and coupled model applications (5.0.0), Zenodo. https://doi.org/10.5281/zenodo.4893099, 2021.

Hagemann, S., Stacke, T., and Ho-Hagemann, H.T.M.: High resolution discharge simulations over Europe and the Baltic Sea catchment, Frontiers in Earth Science, 8, https://doi.org/10.3389/feart.2020.00012, 2020.

Hagemann, S., Stacke, T.: Complementing ERA5 and E-OBS with high-resolution river discharge over Europe. Oceanologia 65: 230-248, doi:10.1016/j.oceano.2022.07.003, 2022.

Hagemann, S., Ho-Hagemann, H. T. M., and Hanke, M.: The Hydrological Discharge Model - a river runoff component for offline and coupled model applications (5.2.2), Zenodo, https://doi.org/10.5281/zenodo.10405875, 2023.

Hanke, M., Redler, R., Holfeld, T., and Yastremsky, M.: YAC 1.2.0: new aspects for coupling software in Earth system modelling, Geosci. Model Dev., 9, 2755-2769, https://doi.org/10.5194/gmd-9-2755-201, 2016.

Haylock, M., Hofstra, N., Klein Tank, A., Klok, E., Jones, P., and New, M.: A European daily high-resolution gridded data set of surface temperature and precipitation for 1950–2006, J. Geophys. Res.-Atmos., 113, D20119, https://doi.org/10.1029/2008JD010201, 2008.

Heinze, R., Dipankar, A., Henken, C. C., Moseley, C., Sourdeval, O., Trömel, S., Xie, X., Adamidis, P., Ament, F., Baars, H., Barthlott, C., Behrendt, A., Blahak, U., Bley, S., Brdar, S., Brueck, M., Crewell, S., Deneke,H., Di Girolamo,P., Evaristo, R., Fischer, J., Frank, C., Friederichs, P., Göcke, T., Gorges, K., Hande, L., Hanke, M., Hansen, A., Hege, H-C., Hoose, C., Jahns, T., Kalthoff, N., Klocke, D., Kneifel, S., Knippertz, P., Kuhn, A., van Laar, T., Macke, A., Maurer, V., Mayer, B., Meyer, C. I., Muppa, S. K., Neggers, R. A. J., Orlandi, E., Pantillon, F., Pospichal, B., Röber,N., Scheck, L., Seifert, A., Seifert, P., Senf, F., Siligam, P., Simmer, C., Steinke, S., Stevens, B., Wapler, K., Weniger, M.,Wulfmeyer, V., Zängl, G., Zhang, D., and Quaas, J.: Large-eddy simulations over Germany using ICON: A comprehensive evaluation, Q. J. Roy. Meteor. Soc., 143, 69–100, 2017.

Hersbach, H., Bell, B., Berrisford, P., Hirahara, S., Horányi, A., Muñoz Sabater, J., et al.: The ERA5 global reanalysis, Q. J. Roy. Meteor. Soc., 146(730), 1999-2049. https://doi.org/10.1002/qj.3803, 2020.

Hill, C., DeLuca, C., Balaji, Suarez, M., and Da Silva, A.: The architecture of the Earth System Modeling Framework, Computing in Science Engineering, 6, 18–28, https://doi.org/10.1109/MCISE.2004.1255817, 2004.

Hogan, R. J., and Bozzo, A.: A flexible and efficient radiation scheme for the ECMWF model. J. Adv. Model Earth Sys., 10(8), 1990–2008, 2018.

Ho-Hagemann, H. T. M.: The OASIS3-MCT Coupling Interface for ICON-CLM (1.0.0). Zenodo. https://doi.org/10.5281/zenodo.5833118, 2022.

Ho-Hagemann, H. T. M.: Regional Earth system model GCOAST-AHOI v2.0 with ICON-CLM (1.0.1). Zenodo. https://doi.org/10.5281/zenodo.11057794, 2024.

Ho-Hagemann, H. T. M., Hagemann, S., and Rockel, B.: On the role of soil moisture in the generation of heavy rainfall during the Oder flood event in July 1997, Tellus A 2015, 67, 28661, https://doi.org/10.3402/tellusa.v67.28661, 2015.

Ho-Hagemann, H. T. M., Gröger, M., Rockel, B., Zahn, M., Geyer, B., and Meier, H. E. M.: Effects of air-sea coupling over the North Sea and the Baltic Sea on simulated summer precipitation over Central Europe, Clim Dyn 49, 3851-3876. https://doi.org/10.1007/s00382-017-3546-8, 2017.

Ho-Hagemann, H. T. M., Hagemann, S., Grayek, S., Petrik, R., Rockel, B., Staneva, J., Feser, F., and Schrum, C.: Internal model variability of the regional coupled system model GCOAST-AHOI, Atmosphere, 11(3), 227. https://doi.org/10.3390/atmos11030227, 2020.

Jungclaus, J. H., Lorenz, S. J., Schmidt, H., Brovkin, V., Brüggemann, N., Chegini, F., et al.: The ICON Earth System Model version 1.0. Journal of Advances in Modeling Earth Systems, 14, e2021MS002813.

https://doi.org/10.5194/egusphere-2024-923
Preprint. Discussion started: 26 April 2024

https://doi.org/10.1029/2021MS002813, 2022.

Kinne, S.: Aerosol radiative effects with MACv2, Atmos. Chem. Phys., 19, 10919–10959, https://doi.org/10.5194/acp-19-10919-2019, 2019.

Korn, P.: Formulation of an unstructured grid model for global ocean dynamics. Journal of Computational Physics, 339, 525–552. https://doi.org/10.1016/j.jcp.2017.03.009, 2017.

Large, W. G., and S. Yeager: Diurnal to decadal global forcing for ocean and sea-ice models: the data sets and flux climatologies, NCAR Technical Note, NCAR/TN-460+STR, CGD Division of the National Center for Atmospheric Research, 2004.

Lewis, H.W., Castillo Sanchez, J.M., Siddorn, J., King, R.R., Tonani, M., Saulter, A., Sykes, P., Pequignet, A.-C., Weedon, G.P., Palmer, T., Staneva, J., and Bricheno, L.: Can wave coupling improve operational regional ocean forecasts for the north-west European Shelf?, Ocean Sci., 15, 669-690, https://doi.org/10.5194/os-15-669-2019, 2019.

Lemmen, C., Hofmeister, R., Klingbeil, K., Nasermoaddeli, M.H., Kerimoglu, O., Burchard, H., Kösters, F., and Wirtz, K.W.: Modular System for Shelves and Coasts (MOSSCO v1.0) – a flexible and multi-component framework for coupled coastal ocean ecosystem modelling, Geosci. Model Dev., 11, 915-935, https://doi.org/10.5194/gmd-11-915-2018, 2018.

Madec, G., Bourdallé-Badie, R., Bouttier, P.-A., Bricaud, C., Bruciaferri, D., Calvert, D., Chanut, J., Clementi, E., Coward, A., Delrosso, D., Ethé, C., Flavoni, S., Graham, T., Harle, J., Iovino, D., Lea, D., Lévy, C., Lovato, T., Martin, N., Masson, S., Mocavero, S., Paul, J., Rousset, C., Storkey, D., Storto, A., and Vancoppenolle, M.: NEMO ocean engine (Version v3.6-patch), Tech. rep., Pôle De Modélisation De L'institut Pierre-simon Laplace (IPSL), Zenodo, https://doi.org/10.5281/ZENODO.3248739, 2017.

Maisonnave E., and Caubel A.: LUCIA, load balancing tool for OASIS coupled systems, https://cerfacs.fr/wp-content/uploads/2018/10/GLOBC_TR_Maisonnave_lucia_arnaud_2014.pdf, 2014.

Pein, J., Eisele, A., Hofmeister, R., Sanders, T., Daewel, U., Stanev, E.V., van Beusekom, J., Staneva, J., and Schrum, C.: Nitrogen cycling in the Elbe estuary from a joint 3D-modelling and observational perspective, Biogeosciences Discuss., (July), 1–34, https://doi.org/10.5194/bg-2019-265, 2019.

Pfeifroth, U., Kothe, S., Müller, R., Trentmann, J., Hollmann, R., Fuchs, P., and Werscheck, M.: Surface Radiation Data Set – Heliosat (SARAH) – Edition 2, Satellite Application Facility on Climate Monitoring, https://doi.org/10.5676/EUM_SAF_CM/SARAH/V002, 2017.

Pham, T. V., Steger, C., Rockel, B., Keuler, K., Kirchner, I., Mertens, M., Rieger, D., Zängl, G., and Früh, B.: ICON in Climate Limited-area Mode (ICON release version 2.6.1): a new regional climate model, Geosci. Model Dev., 14, 985–1005, https://doi.org/10.5194/gmd-14-985-2021, 2021.

Raupach, M.R., and Shaw, R.H.: Averaging procedures for flow within vegetation canopies. Boundary-Layer Meteorol 22, 79–90. https://doi.org/10.1007/BF00128057, 1982.

Raschendorfer, M.: The new turbulence parameterization of LM. In: G. Doms and U. Schättler (Edts.): COSMO Newsletter No. 1, 89-97 (available at www.cosmo-model.org), 2001.

Reick, C., V. Gayler, D. Goll, and S. Hagemann et al.: JSBACH 3 - The land component of the MPI Earth System Model: Documentation of version 3.2, Berichte zur Erdsystemforschung, 240, Max Planck Institute for Meteorology, Hamburg, http://doi.org/10.17617/2.3279802, 2021.

Rieger, D., Köhler, M., Hogan, R., Schäfer, S., Seifert, A., Lozar, A. D., and Zängl, G.: ecRad in ICON – Implementation Overview, Reports on ICON, Deutscher Wetterdienst, Offenbach, Germany, https://doi.org/10.5676/DWDpub/nwv/icon004, 2019.

Rockel, B., and Geyer, B.: SPICE (Starter Package for ICON-CLM Experiments) (2.1), Zenodo. https://doi.org/10.5281/zenodo.7298390, 2022.

Rockel, B., Will, A., and Hense, A.: The regional climate model COSMO-CLM (CCLM), Meteorol. Z. 2008, 17, 347–348. doi:10.1127/0941-2948/2008/0309, 2008.

Russo, E., Geyer, B., Petrik, P., Keuler, K., Adinol, M., Feldmann, H., Goergen, K., Kerkweg, A., Khain, P., Ludwig, P., Mertens, M., Pothapakula, P., Raffa, M., Rockel, B., Schulz, J.-P., Sulis, M., Ho-Hagemann, H. T. M., Truhetz, H., Uzan, L., Voggenberger, U., and Steger, C.: CLM Community WG EVAL, COordinated Parameter Testing project 2 (COPAT2): COSMO-CLM 6.0 clm1 recommended model configuration, COSMO Technical Reports, No. 51, https://doi.org/10.5676/DWD_pub/nwv/cosmo-tr_51, 2024.

Schloen, J., Stanev, E.V., and Grashorn, S.: Wave-current interactions in the southern North Sea: The impact on salinity. Ocean Modelling 111 (2017) 19–37, https://doi.org/10.1016/j.ocemod.2017.01.003, 2017.

Schrodin, R., and Heise, E.: The multi-layer-version of the DWD soil model TERRA/LM. Consortium for Small-

Scale Modelling (COSMO) Tech. Rep., 2, 16, 2001.
Shrestha, P., Sulis, M., Masbou, M., Kollet, S., and Simmer, C.: A scale-consistent terrestrial systems modeling platform based on COSMO, CLM, and ParFlow, Mon. Weather Rev., 142, 3466–3483, 2014.
Schulz, J.-P., Vogel, G., Becker, C., Kothe, S., Rummel, U., Ahrens, B.: Evaluation of the ground heat flux simulated by a multi-layer land surface scheme using high-quality observations at grass land and bare soil Meteorol. Z., 25, pp. 607-620, https://doi.org/10.1127/metz/2016/0537, 2016.
Schulz, J.-P., and Vogel, G.: Improving the processes in the land surface scheme TERRA: bare soil evaporation and skin temperature Atmosphere, 11, p. 513, https://doi.org/10.3390/atmos11050513, 2020.
Slavik, K., Lemmen, C., Zhang, W., Kerimoglu, O., Klingbeil, K., and Wirtz, K.W. The large scale impact of offshore windfarm structures on pelagic primary production in the southern North Sea, Hydrobiologia (2019) 845: 35, https://doi.org/10.1007/s10750-018-3653-5, 2019.
Staneva, J., Alari, V., Breivik, Ø., Bidlot, J.-R., and Mogensen, K.: Effects of wave-induced forcing on a circulation model of the North Sea, Ocean Dynamics, https://doi.org/10.1007/s10236-016-1009-0, 2016.
Staneva, J., Schrum, C., Behrens, A., Grayek, S., Ho-Hagemann, H., Alari, V., Breivik, Ø., and Bidlot, J.-R.: A North Sea - Baltic Sea regional coupled models: atmosphere, wind, waves and ocean. In: Buch, E., Fernández, V., Eparkhina, D., Gorringe, P., and Nolan, G. (Eds.): Operational Oceanography serving Sustainable Marine Development, Proceedings of the Eight EuroGOOS International Conference, 516 pp, ISBN 978-2-9601883-3-2, 2018.
Schrodin, R., and Heise, E.: The multi-layer-version of the DWD soil model TERRA/LM. Consortium for Small-Scale Modelling (COSMO) Tech. Rep 2001, 2, 16, 2001.
Tegen, I., P. Hollrigl, M. Chin, I. Fung, D. Jacob, and Penner, J.: Contribution of different aerosol species to the global aerosol extinction optical thickness: Estimates from model results, J. Geophys. Res., 102, 23895-23915, 1997.
Tiedtke, M. A comprehensive mass flux scheme for cumulus parameterization in large-scale models. Mon. Weather Rev. 1989, 117, 1779–1800.
Valcke, S., Craig, T., and Coquart, L.: OASIS3-MCT user guide, OASIS3-MCT 3.0. Technical Report TR/CMGC/15/38, CERFACS, Toulouse, France, CERFACS/CNRS SUC URA No 1875, 2015.
Van den Besselaar, E., Haylock, M., Van der Schrier, G., and Klein Tank, A.: A European daily high-resolution observational gridded data set of sea level pressure, J. Geophys. Res.-Atmos., 116, D11110, https://doi.org/10.1029/2010JD015468, 2011.
Wahle, K., Staneva, J., Koch, W., Fenoglio-Marc, L., Ho-Hagemann, H.T.M., and Stanev, E.V.: An atmosphere–wave regional coupled model: improving predictions of wave heights and surface winds in the southern North Sea, Ocean Sci., 13, 289-301, https://doi.org/10.5194/os-13-289-2017, 2017.
Wiese, A., Staneva, J., Ho-Hagemann, H. T. M., Grayek, S., Koch, W., and Schrum, C.: Internal Model Variability of Ensemble Simulations with a Regional Coupled Wave-Atmosphere Model GCOAST, Frontiers in Marine Science, 7, 596843, https://doi.org/10.3389/fmars.2020.596843, 2020.
Wiese, A., Stanev, E., Koch, W., Behrens, A., Geyer, B., and Staneva, J.: The Impact of the Two-Way Coupling between Wind Wave and Atmospheric Models on the Lower Atmosphere over the North Sea, Atmosphere 2019, 10, 386, https://doi.org/10.3390/atmos10070386, 2019.
Will, A., Akhtar, N., Brauch, J., Breil, M., Davin, E., Ho-Hagemann, H.T.M., Maisonnave, E., Thürkow, M., and Weiher, S.: The COSMO-CLM 4.8 regional climate model coupled to regional ocean, land surface and global earth system models using OASIS3-MCT: Description and performance, Geosci. Model Dev. 2017, 10, 1549–1586. doi:10.5194/gmd-10-1549-2017, 2017.
Zängl, G., Reinert, D., Rípodas, P., and Baldauf, M.: The ICON (ICOsahedral Non-hydrostatic) modelling framework of DWD and MPI-M: Description of the non-hydrostatic dynamical core, Q. J. Roy. Meteor. Soc., 141, 563–579, https://doi.org/10.1002/qj.2378, 2015.
Zhang, W., Wirtz, K., Daewel, U., Wrede, A., Kröncke, I., Kuhn, G., Neumann, A., Meyer, J., Ma, M., and Schrum, C.: The budget of macrobenthic reworked organic carbon - a modelling case study of the North Sea, Journal of Geophysical Research-Biogeosciences, https://doi.org/10.1029/2019JG005109, 2019.